CHEST

Shape-Sensing Robotic-Assisted Bronchoscopy in the Diagnosis of Pulmonary Parenchymal Lesions

Or Kalchiem-Dekel, MD; James G. Connolly, MD; I-Hsin Lin, PhD; Bryan C. Husta, MD, FCCP; Prasad S. Adusumilli, MD; Jason A. Beattie, MD; Darren J. Buonocore, MD; Joseph Dycoco, BS; Paige Fuentes, MS; David R. Jones, MD; Robert P. Lee, MD, FCCP; Bernard J. Park, MD, FCCP; Gaetano Rocco, MD, FCCP; Mohit Chawla, MD, FCCP; and Matthew J. Bott, MD

BACKGROUND: The landscape of guided bronchoscopy for the sampling of pulmonary parenchymal lesions is evolving rapidly. Shape-sensing robotic-assisted bronchoscopy (ssRAB) recently was introduced as means to allow successful sampling of traditionally challenging lesions.

RESEARCH QUESTION: What are the feasibility, diagnostic yield, determinants of diagnostic sampling, and safety of ssRAB in patients with pulmonary lesions?

STUDY DESIGN AND METHODS: Data from 131 consecutive ssRAB procedures performed at a US-based cancer center between October 2019 and July 2020 were captured prospectively and analyzed retrospectively. Definitions of diagnostic procedures were based on prior standards. Associations of procedure- and lesion-related factors with diagnostic yield were examined by univariate and multivariate generalized linear mixed models.

RESULTS: A total of 159 pulmonary lesions were targeted during 131 ssRAB procedures. The median lesion size was 1.8 cm, 59.1% of lesions were in the upper lobe, and 66.7% of lesions were beyond a sixth-generation airway. The navigational success rate was 98.7%. The overall diagnostic yield was 81.7%. Lesion size of $\geq$ 1.8 cm and central location were associated significantly with a diagnostic procedure in the univariate analysis. In the multivariate model, lesions of $\geq$ 1.8 cm were more likely to be diagnostic compared with lesions $<$ 1.8 cm, after adjusting for lung centrality (OR, 12.22; 95% CI, 1.66-90.10). The sensitivity and negative predictive value of ssRAB for primary thoracic malignancies were 79.8% and 72.4%, respectively. The overall complication rate was 3.0%, and the pneumothorax rate was 1.5%.

INTERPRETATION: This study was the first to provide comprehensive evidence regarding the usefulness and diagnostic yield of ssRAB in the sampling of pulmonary parenchymal lesions. ssRAB may represent a significant advancement in the ability to access and sample successfully traditionally challenging pulmonary lesions via the bronchoscopic approach, while maintaining a superb safety profile. Lesion size seems to remain the major predictor of a diagnostic procedure.

CHEST 2022; 161(2):572-582

KEY WORDS: diagnostic yield; pulmonary nodule; robotic-assisted bronchoscopy

ABBREVIATIONS: EBUS = endobronchial ultrasound; EMN = electromagnetic navigation; FN = false-negative; IQR = interquartile range; RAB = robotic-assisted bronchoscopy; rEBUS = radial probe endobronchial ultrasound; ROSE = rapid on-site evaluation; ssRAB = shape-sensing robotic-assisted bronchoscopy

AFFILIATIONS: From the Section of Interventional Pulmonology (O. Kalchiem-Dekel, B. C. Husta, J. A. Beattie, P. Fuentes, R. P. Lee, and M. Chawla), Pulmonary Service, Department of Medicine, the Thoracic Service (J. G. Connolly, P. S. Adusumilli, J. Dycoco, D. R. Jones, B. J. Park, G. Rocco, and M. J. Bott), Department of Surgery, the

Take-home Points

Study Question: What is the feasibility, diagnostic yield, determinants of diagnostic sampling, and safety profile of shape-sensing robotic-assisted bronchoscopy (ssRAB) in the sampling of pulmonary parenchymal lesions?

Results: ssRAB allowed successful navigation in 98.7% and diagnostic sampling in 81.7% of lesions, with an overall complication rate of 3.0%. Lesion size was the major predictor of diagnostic sampling.

Interpretation: ssRAB represents an advancement in the ability to access and sample adequately pulmonary lesions bronchoscopically, while maintaining a superb safety profile.

The introduction of the flexible bronchoscope by Ikeda et al[1] in 1966 revolutionized physicians' ability to access and sample pulmonary parenchymal lesions. The set of tools that allow navigation, confirmation of target proximity, and acquisition of tissue is collectively known as *guided bronchoscopy*.[2] The fundamental components of guided bronchoscopy are image-based airway navigation, real-time airway visualization, intraoperative confirmatory imaging, and specimen acquisition tools.

Pivotal prospective trials mapped the strengths and weaknesses of guided bronchoscopy in its various iterations.[3-11] These studies defined diagnostic yield, provided safety data, and contrasted guided bronchoscopy with percutaneous sampling.[12] Although shown to be safer relative to transthoracic sampling,[12,13] the diagnostic yield of guided bronchoscopy historically has ranged between 44% and 74%,[3-11] compared with rates of > 90% for percutaneous sampling.[12,13]

In an attempt to overcome these limitations, two robotic-assisted bronchoscopy (RAB) platforms were developed and received Food and Drug Administration clearance.[14,15] The Monarch RAB platform (Auris Health, Inc.) is based on electromagnetic navigation (EMN) technology,[16,17] whereas the Ion Robotic-Assisted Endoluminal Platform (Intuitive Surgical, Inc.) is based on novel shape-sensing RAB (ssRAB) technology.[18,19] RAB is designed to allow endobronchial navigation into the lung periphery while maintaining catheter stability and shape to maximize precision in sampling.[18] These advantages of RAB were demonstrated previously in cadaveric models.[20-23] In vivo, a study of EMN RAB reported a navigation success rate of 88.6% and a diagnostic yield of 69.1%.[24] A recent study combining RAB with cone-beam CT imaging indicated a diagnostic yield of 83%.[25] These studies also suggested that the diagnostic accuracy of RAB may not be as significantly affected by factors that traditionally have been shown to attenuate the diagnostic yield of bronchoscopic sampling, such as lesion size, radiographic consistency, and lobar location.[3-11]

To date, reported experience with ssRAB is limited to cadaveric studies[21,23] and small studies in humans.[25,26] In this article, we describe our experience with ssRAB sampling of pulmonary lesions by members of a collaborative team of interventional pulmonologists and thoracic surgeons. In this postmarketing report, we provide data on the safety profile of this method and evaluate its diagnostic yield in a high-volume US cancer center.

Methods

Study Design

Patients referred to the Memorial Sloan Kettering Cancer Center interventional pulmonology or thoracic surgery services for evaluation of pulmonary lesions were assessed individually by the proceduralist for clinical need for tissue sampling and adequacy for ssRAB. Adequacy for ssRAB was considered based on clinical assessment and review of the preprocedural CT scan for an airway-lesion relationship that would allow sampling. All cases referred for ssRAB between October 1, 2019, and July 31, 2020, were captured prospectively and analyzed retrospectively. ssRAB procedures that were performed for diagnostic sampling of one or more pulmonary lesions were included in the final analysis. Of 152 patients who underwent evaluation, ssRAB was performed in 132 patients. A single patient who underwent ssRAB for the sole purpose of anchored beacon transponder[27] placement was excluded. The final analysis included a total of 159 parenchymal lung lesions targeted

Department of Epidemiology and Biostatistics (I. Lin), and the Thoracic Pathology Service (D. J. Buonocore), Department of Pathology, Memorial Sloan Kettering Cancer Center, New York, NY.

Drs Chawla and Bott contributed equally to this manuscript as co-senior authors.

Parts of this article were presented during the International Thoracic Surgical Oncology Summit of the American Association for Thoracic Surgery, Toronto, Canada; September 28, 2019.

FUNDING/SUPPORT: This research was funded in part through the National Cancer Institute, National Institutes of Health [Grants P30 CA008748 (all authors), and 1K08CA245206 (to M. J .B.)], and the National Institutes of Health [Grant T32CA009501 (to J. G. C.)]. Additional support was provided through the Fiona and Stanley Druckenmiller Center for Lung Cancer Research and a gift from the late Mr. David H. Koch.

CORRESPONDENCE TO: Mohit Chawla, MD, FCCP; email: chawlam1@mskcc.org

DOI: https://doi.org/10.1016/j.chest.2021.07.2169

by 131 ssRAB procedures in 130 patients (e-Fig 1). All study data were managed using Research Electronic Data Capture tools[28] hosted on a secured server. This Health Insurance Portability and Accountability Act-compliant study was approved by the Memorial Sloan Kettering Cancer Center Institutional Review Board (Identifier: 20-166).

Lesion Characterization and Target Sampling

Pulmonary parenchymal lesions were defined as those bordered by lung parenchyma, requiring transbronchial sampling, not accessible by conventional bronchoscopy, or a combination thereof.[4,29,30] The widest lesion diameter and consistency were documented based on the planning CT imaging in the axial, coronal, and sagittal projections.[29] Centrality was defined as described previously by dividing the lung parenchyma into inner two-thirds and outer one-third.[31,32] An airway leading into the lesion or coursing through as so-called air bronchogram designated a positive bronchus sign.[33] The number of traversed airways during navigation was based on the scheme proposed by Weibel[34] and derived from ssRAB planning.

ssRAB was performed using the Ion Robotic-Assisted Endoluminal Platform, as described previously.[21] CT scan-based planning was conducted using PlanPoint software (Intuitive Surgical). All procedures were performed in a dedicated suite by an interventional pulmonologist or a thoracic surgeon. Each physician sampled a minimum of 10 lesions during the study period (range, 10-47 lesions).[22] The anesthesia protocol used during ssRAB is described in e-Appendix 1. Procedure time was documented from ssRAB arm docking to final undocking. After an initial airway survey with a flexible bronchoscope (BF-P190, BF-1T180, or BF-1TH190; Olympus Corp.), the ssRAB catheter and vision probe were introduced into the airway and registration was performed to synchronize the virtual bronchoscopic view and the real-time camera view. As soon as the catheter was navigated to the target, the vision probe was removed and intraoperative confirmation of proximity to the target was achieved using radial probe endobronchial ultrasound (rEBUS; UM-S20-17S or UM-S20-20R-3; Olympus Corp.), two-dimensional fluoroscopy (OEC 9900 Elite, GE Healthcare Systems), two- and three-dimensional fluoroscopy (Cios-Spin Mobile 3D C-Arm; Siemens Healthineers, Inc.), or a combination thereof. The choice of intraoperative imaging methods was left to the discretion of the operator. rEBUS view was defined as concentric, eccentric, or no-view, as described previously.[35,36] Successful navigation was assessed by the operator and was defined as achieving catheter-target proximity that allowed lesion sampling. Sampling was performed using a 19-, 21-, or 23-gauge Flexision needle (Intuitive Surgical). The choice of needle as well as use of adjunct sampling tools, including biopsy forceps (Captura Bronch Biopsy Forceps; Cook Medical, Inc.; or CoreDx Pulmonary Mini-Forceps; Boston Scientific), cytology brush (Cellebrity; Boston Scientific), BAL, or a combination thereof, was left to the discretion of the operator. Rapid on-site evaluation (ROSE) of cytologic material for adequacy was performed during all procedures.

Outcomes

The primary efficacy outcome of this study was diagnostic yield of ssRAB sampling per individual lesion. In line with previous studies,[5,8,24,30,36,37] three categories of pathologic diagnoses were defined: (1) malignant; (2) nonmalignant, including inflammatory, infectious, and lymphocyte-predominant patterns; and (3) insufficient, including samples lacking sufficient material to infer a diagnosis or showing at most benign bronchial or alveolar tissue. Samples demonstrating atypical cells that could not be classified further were deemed insufficient. Each pathologic diagnostic category then was designated diagnostic or nondiagnostic based on a clinical-radiographic-pathologic correlation algorithm (e-Fig 2): all malignant lesions were considered diagnostic, unless proven false-positive results by a surgical resection, whereas all insufficient samplings were considered nondiagnostic. Nonmalignant lesions were considered diagnostic if: (1) a nonmalignant cause was confirmed by an alternative sampling method, such as transthoracic or surgical biopsy; (2) follow-up imaging demonstrated regression or resolution of the lesion; or (3) the lesion was shown to remain unchanged on follow-up imaging for $\geq$ 1 year.[5,7-11,38] If follow-up imaging revealed an increase in lesion size or stability over $<$ 1 year, or if a clinical decision was made to pursue antineoplastic treatment despite results of the ssRAB sampling, the lesion was classified as a false-negative (FN) finding and hence nondiagnostic.[5,8,11,13,24,29,37] Lesions targeted for ssRAB, but not sampled because of unsuccessful navigation, also were considered nondiagnostic.

Sensitivity and negative predictive value of ssRAB for primary thoracic malignancies were defined as secondary outcomes and were calculated in line with prior studies.[5,8,30] Briefly, all lesion samples that showed positive results for primary thoracic cancer were considered true-positive results, unless proven false-positive results by surgical resection. Lesions that were positive for nonthoracic malignancies were excluded from this analysis. Both nonmalignant and insufficiently sampled lesions were considered FN findings, unless confirmed to be true-negative findings by meeting the diagnostic criteria for nonmalignant lesions (e-Fig 2), that is, confirmed nonmalignant by ancillary sampling, regressed or resolved on follow-up imaging, or remained stable on follow-up imaging for $\geq$ 1 year.

The primary safety outcome of the study was 30-day procedure- or device-related adverse events, including (1) pneumothorax; (2) hemorrhage resulting in early termination of the procedure or intervention that is beyond the use of iced saline, topical epinephrine, or wedging of the bronchoscope; and (3) any increase in the patient's level of care as a direct result of ssRAB.

Statistical Analysis

Descriptive statistics were presented as counts and percentages for categorical variables and as medians and interquartile ranges (IQRs) for continuous variables. The nonparametric Kruskal-Wallis test was used to compare procedure times by number of lesions sampled. The degree of agreement between ROSE and the finalized pathologic interpretation was assessed by Cohen's κ coefficient (e-Appendix 2).[39]

Generalized linear mixed-model analysis for binary data with logit link was performed to evaluate associations between procedure- or lesion-related factors and diagnostic yield with random patient-specific intercepts using diagnostic yield (diagnostic vs nondiagnostic) as a binary outcome; results were reported as P values, OR point estimates, and 95% CIs for the univariate and the multivariate models. The random intercept accounts for correlation of measurements collected on the repeated measures from the same patient. For the univariate and multivariate analyses, the median lesion size of this study's cohort (1.8 cm) was used to differentiate relatively small from relatively large lesions.

All statistical tests were two-tailed, and a P value of $<$ .05 was considered statistically significant. SAS version 9.4 software (SAS Institute, Inc.) was used for all analyses.

Results

Study participants' demographic, anthropometric, and clinical characteristics are summarized in Table 1. The median age was 69 years (IQR, 60-76 years), and 57.5% were women. Most participants were ever smokers (75.4%) and most had a known history of malignancy at the time of the ssRAB procedure (63.8%).

Target Lesions and Procedures

Lesion- and procedure-related data are shown in Table 2. Of lesions targeted, 56.0% were ≤ 2 cm in the largest dimension, 59.1% were located in an upper lobe, and 66.7% were beyond a sixth-generation airway. The CT scan texture of lesions was predominantly solid in 73.0%, pure ground glass in 3.8%, and mixed solid and ground glass in 13.2%. More than one lesion was sampled in 19.0% of procedures (25/131); in 11 cases, bilateral lesions were sampled. The median procedure time was 64 min (IQR, 40-116 min). Procedure time was 49 min (IQR, 35.5-75 min), 71 min (IQR, 64-91 min), and 109 min (IQR, 90-116 min) for one, two, and three lesion samplings, respectively ($P < .001$) (e-Fig 3). Successful navigation to the target was achieved in 98.7% of lesions (157/159) (e-Fig 1). Intraoperative imaging included rEBUS in 85.5%, two-dimensional fluoroscopy in 79.9%, and two- and three-dimensional fluoroscopy in 20.1% of cases. Transbronchial needle aspiration was used in 96.9% of sampling and transbronchial forceps biopsy was used in 32.1%. Linear EBUS evaluation, sampling, or both of thoracic lymph nodes accompanied ssRAB in 54.2% of the procedures.

Diagnostic Yield

The pathologic classification was malignant, nonmalignant, and insufficient in 57.3%, 26.7%, and 16.0% of sampled lesions, respectively. Two lesions were not sampled because of unsuccessful navigation, and hence were defined as nondiagnostic. As illustrated in Figure 1, the overall diagnostic yield was 81.7% (130/159). The diagnostic yield was 66.6%, 70.4%, 92.9%, and 100.0% for lesions ≤ 1.00 cm, 1.01 to 2.00 cm, 2.01 to 3.00 cm, and > 3.00 cm, respectively (Fig 2). The effects of other factors on diagnostic sampling are summarized in e-Tables 1 and 2. The distribution of pathologic interpretations across samplings is illustrated in Figure 3. Of malignant lesions, 83.2% represented primary thoracic malignancies, 73.3% of which were non-small cell lung cancer. Of diagnostic nonmalignant lesions, 67.5% were inflammatory, 25.0% were infectious, and 7.5% represented intrapulmonary lymph nodes (Fig 3). Of the 29 lesions classified as nondiagnostic, 14 (48.3%) were proved malignant by subsequent sampling; 2 (6.9%) were proved nonmalignant by subsequent sampling; 8 (27.5%) regressed, resolved, or remained stable for ≥ 1 year on follow-up imaging; 2 (6.9%) increased in size on follow-up imaging without additional sampling; and 3 (10.4%) had insufficient imaging follow-up to define stability. Of 159 lesions targeted by ssRAB, prior biopsy attempt was performed on 20, 10 of which were via a bronchoscopic approach and 10 of which were by the transthoracic approach. Of the 10 previously insufficient

TABLE 1] Patient Demographic, Anthropometric, and Clinical Characteristics (n = 130)

Variable	Value
Female sex	75 (57.5)
Age, y	69 (60-76)
BMI, kg/m^2	26.7 (23.3-30.6)
Smoking status	
Never smoker	32 (24.6)
Ever smoker	98 (75.4)
Former smoker	86 (66.2)
Current smoker	12 (9.2)
Prior history of cancer	
None	47 (36.2)
Primary thoracic	28 (21.5)
Primary extrathoracic	55 (42.3)
ASA score	
1	0 (0.0)
2	28 (21.6)
3	97 (74.6)
4	5 (3.9)
Comorbidities	
Hypertension	56 (43.1)
COPD	26 (20.0)
CAD	24 (18.5)
Diabetes mellitus	19 (14.6)
Asthma	5 (3.8)
Chronic renal failure	3 (2.3)
Pulmonary hypertension	2 (1.5)
Heart failure	1 (0.8)
Cerebrovascular accident	1 (0.8)
Pulmonary function test indexes	
FEV_1, L	2.2 (1.7-2.6)
FEV_1, % predicted	86.6 (73.0-101.0)
D_{LCO}, % predicted	77.0 (61.0-96.0)

Data are presented as No. (%) or median (interquartile range). ASA = American Society of Anesthesiologists; CAD = coronary artery disease; D_{LCO} = carbon monoxide diffusion capacity.

TABLE 2] Lesion and Procedural Characteristics (N = 159)

Variable	Value
Lesion size, cm	1.8 (1.3-2.7)
Lesion lobar location,	
RUL	53 (33.3)
RML	11 (6.9)
RLL	20 (12.6)
LUL	41 (25.8)
LLL	34 (21.4)
Lung centrality[31,32]	
Inner two-thirds	97 (61.0)
Outer one-third	62 (39.0)
No. of traversed airway generations[34]	7 (6-8)
Bronchus sign[33]	
Positive	100 (62.9)
Negative	59 (37.1)
No. of lesions targeted per procedure	
1	106 (80.9)
2	22 (16.8)
3	3 (2.3)
Procedure time, min	64 (40-116)
Intraoperative imaging	
Radial probe EBUS	136 (85.5)
Radial probe EBUS view	
Concentric	72 (53.0)
Eccentric	52 (38.2)
No view	12 (8.8)
Two-dimensional fluoroscopy	127 (79.9)
Two- and three-dimensional fluoroscopy	32 (20.1)
Sampling method	
TBNA	154 (96.9)
19G	34 (22.0)
21G	56 (36.3)
23G	40 (26.0)
Any combination of two needles	10 (6.5)
Not documented	14 (9.2)
TBFB	51 (32.1)
Transbronchial brushings	4 (2.5)

Data are presented as No. (%) or median (interquartile range). EBUS = endobronchial ultrasound; LLL = left lower lobe; LUL = left upper lobe; RLL = right lower lobe; RML = right middle lobe; RUL = right upper lobe; TBFB = transbronchial forceps biopsy; TBNA = transbronchial needle aspiration.

bronchoscopic biopsies, ssRAB-guided sampling was diagnostic in eight. Of the 10 previously insufficient transthoracic biopsies, ssRAB-guided sampling was diagnostic in six.

The rate of agreement between the ROSE and the finalized pathologic interpretation was 89.9%. The estimate of Cohen's κ coefficient was 0.69, which indicates a substantial agreement ($P < .001$) (e-Table 3). Among all 16 discrepancy cases, the formal pathologic analysis revealed adequate tissue for interpretation, whereas the ROSE concluded that the tissue was inadequate; the final pathologic interpretation was malignant in eight lesions, nonmalignant in seven lesions, and atypical cells in one lesion.

Results of univariate and multivariate generalized linear mixed models are presented in Table 3. In the univariate analysis, lesion size and lung centrality were associated significantly with the diagnostic yield. The bronchus sign status and the rEBUS view did not reach statistical significance in the univariate analysis; however, the point estimate of a positive bronchus sign showed in the expected direction to be a diagnostic predictive factor as compared with a negative bronchus sign. In the multivariate model and after adjusting for lung centrality, lesions of ≥ 1.8 cm were 12.22-fold (95% CI, 1.66-90.10) more likely to be diagnostic compared with lesions < 1.8 cm.

Sensitivity for Primary Thoracic Malignancy

Sensitivity, specificity, negative predictive values, and positive predictive values of ssRAB for primary thoracic malignancies are summarized in e-Table 4. Of 90 malignant lesions diagnosed by ssRAB, 75 were identified as primary thoracic neoplasms, and all were considered to be true-positive results. Of 42 nonmalignant tissue diagnoses, 40 met criteria to be considered true-negative findings, whereas two were considered to be FN findings. Of 27 insufficient tissue samples, 10 met the criteria to be considered as true-negative findings, whereas 17 were considered to be FN findings. In sum, these data reflect a sensitivity of 79.8% and a negative predictive value of 72.4% of ssRAB for primary thoracic malignancies.

Safety

A total of four ssRAB-related adverse events were documented, for a total complication rate of 3.0%. Two patients (1.5%) sustained a pneumothorax, both of which required percutaneous drainage. No instances of significant hemorrhage, airway perforation, or deaths related to ssRAB took place. Data pertaining to adverse events are delineated in e-Table 5.

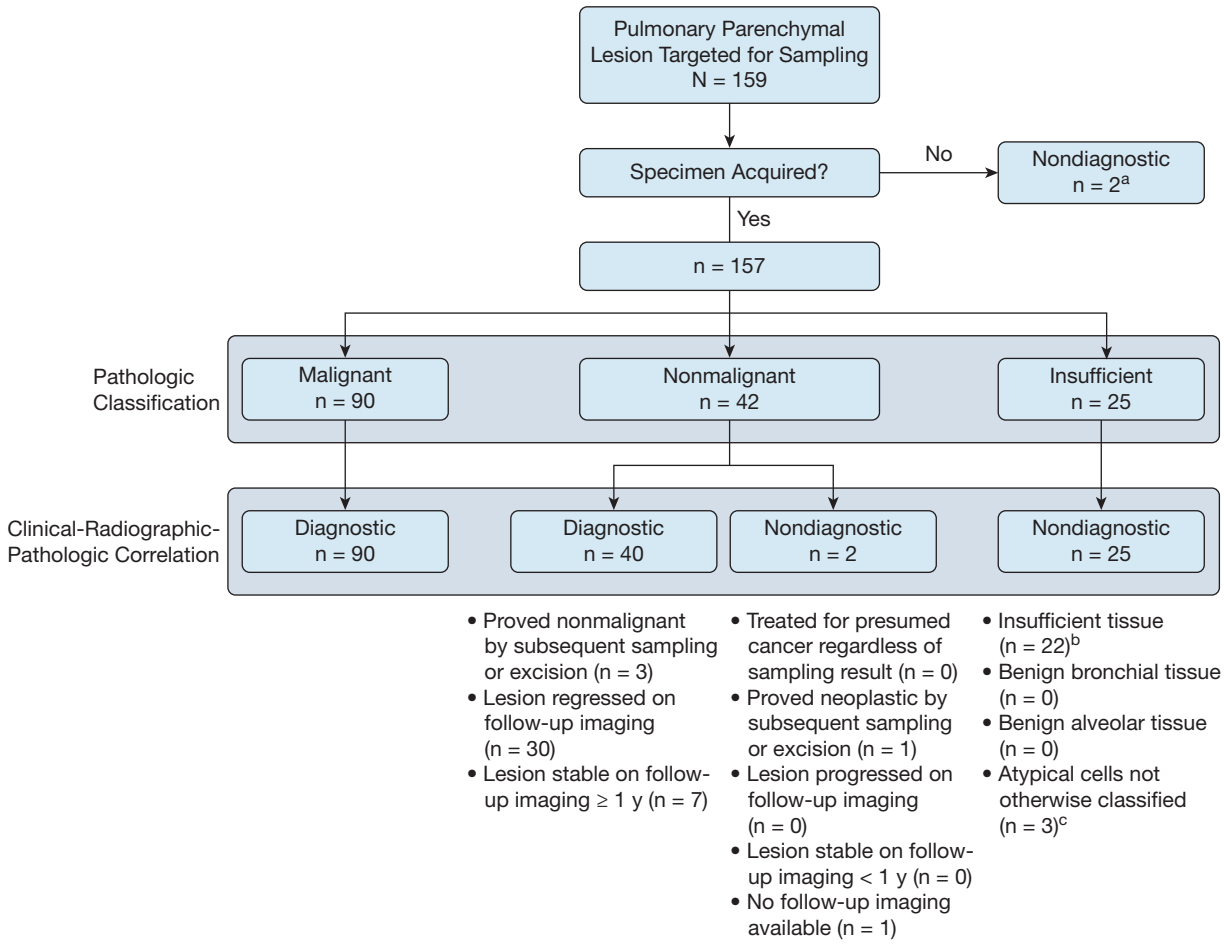

Figure 1 – *Flow chart showing the distribution of diagnostic and nondiagnostic cases as reflected by the diagnostic yield algorithm.* [a]*Both lesions proven malignant by subsequent sampling.* [b]*Nine lesions proven malignant by subsequent sampling, 2 lesions proven benign by subsequent sampling, 7 lesions regressed or resolved on follow-up imaging, 2 lesions increased in size on follow-up imaging, and 2 lesions had insufficient (<1 year) follow-up imaging to confirm stability.* [c]*Two lesions proven malignant by subsequent sampling and one lesion regressed on follow-up imaging.*

Discussion

Guided bronchoscopy continues to evolve with advanced tools that allow successful sampling of smaller and more peripheral lung lesions, while maintaining an advantageous safety profile.[40] These platforms allow consecutive sampling of multiple pulmonary lesions in addition to mediastinal staging by linear EBUS.[41,42] Robotic-assisted bronchoscopy recently was introduced into the armamentarium of guided bronchoscopy tools.[14,15]

In this study, we demonstrated the usefulness of ssRAB in the evaluation of pulmonary parenchymal lesions by a collaborative team of interventional pulmonologists and thoracic surgeons. We provided a rate of diagnostic yield and delineated the clinical, radiographic, and procedure-related factors that impact the degree of diagnostic accuracy. To our knowledge, this is the first study to provide comprehensive postmarketing evidence on the performance of ssRAB within a multidisciplinary clinical practice at a high-volume center.

Previous guided bronchoscopy studies report a wide range of 44% to 74% for diagnostic yield for lung lesions.[7,8,10,30,36] The gap in diagnostic yield between studies can be explained by different definitions of diagnostic tissue, especially in nonmalignant lesions, variability in platforms and tools between and within studies, and a wide range of experience and expertise among operators.[11] Meta-analyses of guided bronchoscopy report a pooled diagnostic accuracy in the range of 70% to 73%[43,44] and pooled sensitivity for lung cancer in the range of 73% to 77%.[43,45,46]

Data on the diagnostic yield of RAB are scarce. In a prospective, multicenter feasibility study of the EMN

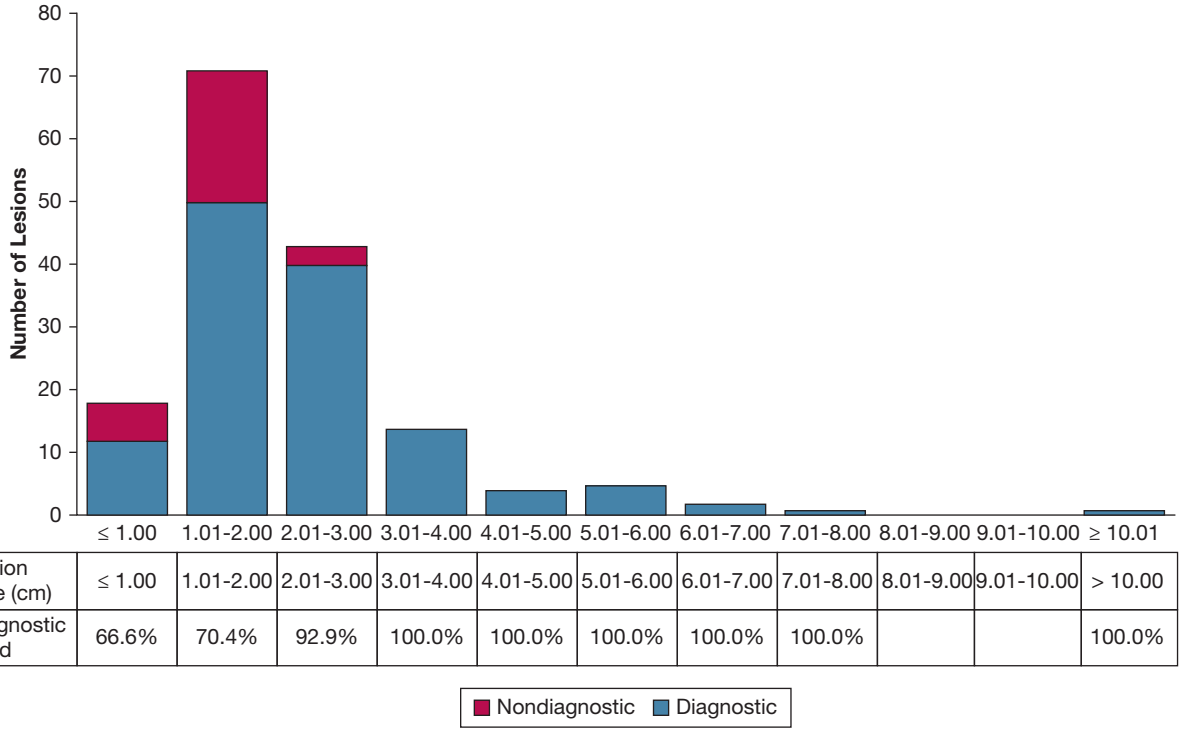

Lesion Size (cm)	≤ 1.00	1.01-2.00	2.01-3.00	3.01-4.00	4.01-5.00	5.01-6.00	6.01-7.00	7.01-8.00	8.01-9.00	9.01-10.00	> 10.00
Diagnostic Yield	66.6%	70.4%	92.9%	100.0%	100.0%	100.0%	100.0%	100.0%			100.0%

Figure 2 – *Bar graph showing diagnostic yield as reflected by the distribution of lesions by size.*

RAB platform on 54 lesions, Chen et al[47] reported successful navigation in 96.2% of lesions and diagnostic sampling in 74.1% of lesions; however, this study was not designed to assess diagnostic yield as a primary outcome. Chaddha et al[24] reported a diagnostic yield of 69.1% with EMN RAB. In this study, determinants of diagnostic yield were the presence of a positive bronchus sign and ability to visualize the target via rEBUS.[24] Benn et al[25] reported a 83% rate of successful acquisition of diagnostic tissue from 59 lung nodules in 52 patients using ssRAB in combination with cone-beam CT imaging. However, this study provided a liberal estimate of diagnostic yield with only limited follow-up data on nonneoplastic nodules.[25]

Our study is distinguished by providing postmarketing experience of a heterogeneous group of interventional pulmonologists and thoracic surgeons along a range of prior expertise in guided bronchoscopy. Our study showed that successful navigation was achieved in 98.7% of the lesions and that the overall diagnostic yield was 81.7%. The major determinant of diagnostic sampling was lesion size. Notably, the diagnostic yield for traditionally challenging lesions of ≤ 2.00 cm in our study was 69.6%, compared with previously reported guided bronchoscopy rates of 43% to 59%.[7,8,11] The diagnostic yield for lesions of > 2.0 cm in our study was 95.7%, which is comparable with that of image-guided transthoracic sampling.[12,13] Our diagnostic yield for traditionally challenging lesions seems to be improved compared with prior studies. For example, the diagnostic yield was 71.1% for lesions with a negative bronchus sign, compared with 43% to 46% in prior studies.[7,8] Similarly, our diagnostic yield for lesions in the outer one-third of the lung was 70.9%, compared with 51.3% as reported by Ost et al.[8] Further, the ssRAB platform allowed us to sample more than one target in 19% of cases, and in a significant proportion of those, bilateral lesions were targeted. Finally, the ssRAB platform provided advantageous overall and pneumothorax safety profiles that are equal[7,8,26,47] or improved[5,24,25] compared with prior guided bronchoscopy studies. Our data demonstrate that although providing an excellent safety profile and improved diagnostic yield compared with prior guided bronchoscopy platforms, less accessible lesions—that is, smaller and peripheral—remain challenging also for the ssRAB platform, albeit with an improved diagnostic yield.

Both currently available RAB platforms include a fully articulating robotic catheter; however, the distinct characteristics of each may not make these platforms

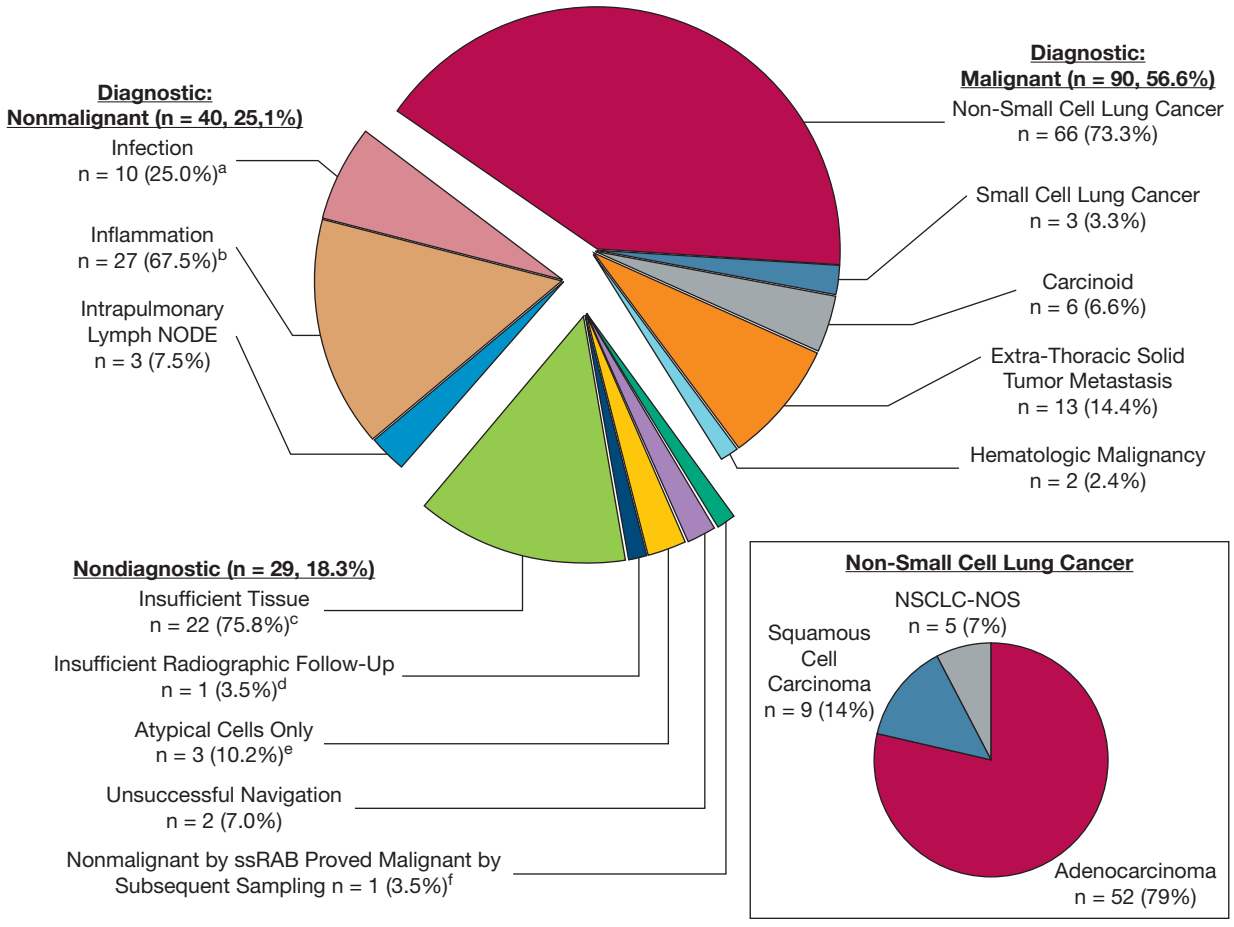

Figure 3 – *Pie chart showing the distribution of lesion diagnoses (N = 159). [a]Isolated organisms included nontuberculous mycobacteria (n = 3), Pseudomonas aeruginosa (n = 2), Nocardia species (n = 2), Aspergillus species (n = 2), Mycobacterium TB (n = 1), Streptococcus pneumoniae (n = 1), and Chryseobacterium species (n = 1). [b]Patterns of inflammation included chronic inflammation (n = 10), granulomatous inflammation (n = 8), organizing pneumonia (n = 3), eosinophilic inflammation (n = 3), and acute or neutrophilic inflammation (n = 3). [c]Of 22 insufficient samplings, 11 proved malignant by subsequent sampling or excision, two proved benign by subsequent sampling or excision, seven regressed or resolved on follow-up imaging, two increased in size on follow-up imaging, and two had insufficient follow-up imaging to define stability. [d]Lesion was compatible with granulomatous inflammation. [e]Of three samplings revealing atypical cells not further classified, two proved malignant by subsequent sampling and one regressed on follow-up imaging. [f]Proven adenocarcinoma of the lung by CT scan-guided transthoracic biopsy. NOS = not otherwise specified; NSCLC = non-small cell lung cancer; ssRAB = shape-sensing robotic-assisted bronchoscopy.*

interchangeable.[40,48] An important difference lies in the navigation and localization technology. ssRAB technology is applied in the form of a fiber that is embedded along the robotic catheter, providing real-time shape and location information that is corroborated with the CT scan-derived airway map throughout navigation and specimen acquisition.[18,26] In contrast, the EMN RAB technology uses an external electromagnetic field generator that localizes and tracks sensors embedded in the robotic catheter and corroborates those signals with the CT scan-derived airway map.[16,17] Other differences pertain to the outer diameter of the distal end of the robotic catheter, working channel size, visualization, and the controller style, as described previously.[48]

This study has several limitations. This is a retrospective observational study conducted in a single, high-volume academic cancer center. Therefore, selection bias is possible with triaging of patients for ssRAB based on favorable imaging characteristics of the target lesion; however, a considerable proportion of the lesions in our study were considered challenging based on prior definitions,[5,7,8,11] that is, < 2.0 cm in widest diameter (67.4%), upper lobe location (59%), peripheral lung (39%), negative bronchus sign (37%), eccentric or no rEBUS view (47%), or a combination thereof. The prevalence of malignancy among our study participants was relatively high, as expected from a cancer center referral population. A cohort enriched by patients with high probability of cancer may increase the diagnostic

TABLE 3] Predictors of Diagnostic Yield of ssRAB in the Sampling of Pulmonary Parenchymal Lesions

	Univariate Model		Multivariate Model	
Factor	OR (95% CI)	*P* Value	OR (95% CI)	*P* Value
Lesions size, cm				
< 1.8	1.0	...	1.0	...
≥ 1.8	21.74 (1.52-311.58)	.03	12.22 (1.66-90.10)	.02
Lung centrality				
Outer one-third	1.0	...	1.0	...
Inner two-thirds	4.58 (1.18-17.76)	.03	3.70 (0.91-15.14)	.07
Bronchus sign				
Negative	1.0	...	. . .	...
Positive	4.79 (0.94-24.56)	.06	...	...
Radial probe EBUS view				
Eccentric	1.0	...	...	...
Concentric	8.98 (0.54-31.55)	.12	...	...

EBUS = endobronchial ultrasound; ssRAB = shape-sensing robotic-assisted bronchoscopy.

yield because bronchoscopy is more sensitive for malignancy than for nonmalignant disease.[43,45] Therefore, our results can be generalized to populations with a relatively high suspicion for cancer. Our study is also limited by the number of participants and target lesions; this may account for the observation that point estimates of the predictors of diagnostic yield were showing in the expected direction, but failed to reach statistical significance in the multivariate model.

Interpretation

To conclude, this study summarizes our initial clinical experience regarding the feasibility, diagnostic accuracy, and safety of ssRAB in the evaluation of 159 pulmonary lesions by a diverse group of bronchoscopists. This is also the first study to report successful collaboration between interventional pulmonologists and thoracic surgeons in establishing and operating a RAB service in a single high-volume academic center. Our data indicate that ssRAB presents a novel approach to access and sample pulmonary lesions successfully, with an overall diagnostic yield of 81.7%, while maintaining an excellent safety profile. In this study, diagnostic yield remained relatively high, albeit attenuated, for lesions that traditionally have been associated with a significantly reduced diagnostic yield, mainly upper lobe and peripheral lesion location. Lesion size remains the main factor predicting a successful procedure; however, compared with prior reports of guided bronchoscopy, our data demonstrate improved diagnostic accuracy of smaller lesions and a diagnostic yield that is comparable with transthoracic biopsy for larger lesions. Prospective, multicenter trials are warranted to delineate further the strengths and limitations of ssRAB.[38] Collectively, our data suggest that ssRAB may offer a significant advancement in the field of guided bronchoscopy, providing an enhanced, accurate, and safe diagnostic method in the evaluation of pulmonary parenchymal lesions.

Acknowledgments

Author contributions: O. K.-D., J. G. C., B. C. H., P. S. A., J. A. B., J. D., D. R. J., R. P. L., B. J. P., G. R., M. C., and M. J. B. contributed to conception and design of the study. O. K.-D., J. G. C., P. F., B. C. H., J. A. B., D. J. B., R. P. L., M. C., and M. J. B. contributed to collection and assembly of data. O. K.-D., I-H. L., M. C., and M. J. B. conducted the data analysis. O. K.-D., D. J. B., I-H. L., M. C., and M. J. B. wrote the manuscript. All authors reviewed and revised the manuscript and gave final approval of the manuscript. M. C. and M. J. B. are the study guarantors.

Financial/nonfinancial disclosures: The authors have reported to *CHEST* the following: B. C. H., B. J. P., M. J. B., and R. P. L. report receiving speaker fees from Intuitive Surgical, Inc. D. J. B. reports receiving consulting fees from Janssen Pharmaceuticals, Inc. D. J. R. reports receiving advisory fees from AstraZeneca, Inc., and is a member of the clinical trial steering committee of Merck, Inc. G. R. reports receiving royalties from Scanlan International Surgical Instruments, Inc. None declared (O. K.-D., J. G. C., I-H. L., P. S. A., J. A. B., J. D., P. F., G. R., M. C.).

Role of sponsors: The sponsor had no role in the design of the study, the collection and analysis of the data, or the preparation of the manuscript.

Additional information: The e-Appendixes, e-Figures, and e-Tables can be found in the Supplemental Materials section of the online article.

References

1. Ikeda S, Yanai N, Ishikawa S. Flexible bronchofiberscope. *Keio J Med*. 1968;17(1):1-16.
2. Panchabhai TS, Mehta AC. Historical perspectives of bronchoscopy. Connecting the dots. *Ann Am Thorac Soc*. 2015;12(5):631-641.
3. Asano F, Shinagawa N, Ishida T, et al. Virtual bronchoscopic navigation combined with ultrathin bronchoscopy. A randomized clinical trial. *Am J Respir Crit Care Med*. 2013;188(3):327-333.
4. Eberhardt R, Anantham D, Ernst A, Feller-Kopman D, Herth F. Multimodality bronchoscopic diagnosis of peripheral lung lesions: a randomized controlled trial. *Am J Respir Crit Care Med*. 2007;176(1):36-41.
5. Folch EE, Pritchett MA, Nead MA, et al. Electromagnetic navigation bronchoscopy for peripheral pulmonary lesions: one-year results of the prospective, multicenter NAVIGATE Study. *J Thorac Oncol*. 2019;14(3):445-458.
6. Gildea TR, Mazzone PJ, Karnak D, Meziane M, Mehta AC. Electromagnetic navigation diagnostic bronchoscopy: a prospective study. *Am J Respir Crit Care Med*. 2006;174(9):982-989.
7. Oki M, Saka H, Ando M, et al. Ultrathin bronchoscopy with multimodal devices for peripheral pulmonary lesions. A randomized trial. *Am J Respir Crit Care Med*. 2015;192(4):468-476.
8. Ost DE, Ernst A, Lei X, et al. Diagnostic yield and complications of bronchoscopy for peripheral lung lesions. Results of the AQuIRE Registry. *Am J Respir Crit Care Med*. 2016;193(1):68-77.
9. Silvestri GA, Vachani A, Whitney D, et al. A bronchial genomic classifier for the diagnostic evaluation of lung cancer. *N Engl J Med*. 2015;373(3):243-251.
10. Tanner NT, Yarmus L, Chen A, et al. Standard bronchoscopy with fluoroscopy vs thin bronchoscopy and radial endobronchial ultrasound for biopsy of pulmonary lesions: a multicenter, prospective, randomized trial. *Chest*. 2018;154(5):1035-1043.
11. Silvestri GA, Bevill BT, Huang J, et al. An evaluation of diagnostic yield from bronchoscopy: the impact of clinical/radiographic factors, procedure type, and degree of suspicion for cancer. *Chest*. 2020;157(6):1656-1664.
12. DiBardino DM, Yarmus LB, Semaan RW. Transthoracic needle biopsy of the lung. *J Thorac Dis*. 2015;7(suppl 4):S304-S316.
13. Bhatt KM, Tandon YK, Graham R, et al. Electromagnetic navigational bronchoscopy versus CT-guided percutaneous sampling of peripheral indeterminate pulmonary nodules: a cohort study. *Radiology*. 2018;286(3):1052-1061.
14. United States Food and Drug Administration. 510(k) Premarket notification—Monarch Endoscopy Platform (Monarch Platform). March 22, 2018. Food and Drug Administration website. https://www.accessdata.fda.gov/scripts/cdrh/cfdocs/cfpmn/pmn.cfm?ID=K173760. Accessed May 9, 2020.
15. United States Food and Drug Administration. 510(k) Premarket notification—Ion Endoluminal System. November 26, 2019. Food and Drug Administration website. https://www.accessdata.fda.gov/scripts/cdrh/cfdocs/cfpmn/pmn.cfm?ID=K192367. Accessed May 9, 2020.
16. Solomon SB, White P Jr, Acker DE, Strandberg J, Venbrux AC. Real-time bronchoscope tip localization enables three-dimensional CT image guidance for transbronchial needle aspiration in swine. *Chest*. 1998;114(5):1405-1410.
17. Rojas-Solano JR, Ugalde-Gamboa L, Machuzak M. Robotic bronchoscopy for diagnosis of suspected lung cancer: a feasibility study. *J Bronchology Interv Pulmonol*. 2018;25(3):168-175.
18. Galloway KC, Chen Y, Templeton E, Rife B, Godage IS, Barth EJ. Fiber optic shape sensing for soft robotics. *Soft Robot*. 2019;6(5):671-684.
19. Poeggel S, Tosi D, Duraibabu D, Leen G, McGrath D, Lewis E. Optical fibre pressure sensors in medical applications. *Sensors (Basel)*. 2015;15(7):17115-17148.
20. Chen AC, Gillespie CT. Robotic endoscopic airway challenge: REACH assessment. *Ann Thorac Surg*. 2018;106(1):293-297.
21. Yarmus L, Akulian J, Wahidi M, et al. A prospective randomized comparative study of three guided bronchoscopic approaches for investigating pulmonary nodules: the PRECISION-1 Study. *Chest*. 2020;157(3):694-701.
22. Chen AC, Pastis NJ, Machuzak MS, et al. Accuracy of a robotic endoscopic system in cadaver models with simulated tumor targets: ACCESS study. *Respiration*. 2020;99(1):56-61.
23. Kapp CM, Akulian JA, Yu DH, et al. Cognitive load association for electromagnetic navigational and robotic-assisted bronchoscopy for pulmonary nodules, *ATS Sch*. 2020;2(1):97-107.
24. Chaddha U, Kovacs SP, Manley C, et al. Robot-assisted bronchoscopy for pulmonary lesion diagnosis: results from the initial multicenter experience. *BMC Pulm Med*. 2019;19(1):243-249.
25. Benn BS, Romero AO, Lum M, Krishna G. Robotic-assisted navigation bronchoscopy as a paradigm shift in peripheral lung access. *Lung*. 2021;199(2):177-186.
26. Fielding DIK, Bashirzadeh F, Son JH, et al. First human use of a new robotic-assisted fiber optic sensing navigation system for small peripheral pulmonary nodules. *Respiration*. 2019;98(2):142-150.
27. Zhang P, Hunt M, Telles AB, et al. Design and validation of a MV/kV imaging-based markerless tracking system for assessing real-time lung tumor motion. *Med Phys*. 2018;45(12):5555-5563.
28. Harris PA, Taylor R, Minor BL, et al. The REDCap consortium: building an international community of software platform partners. *J Biomed Inform*. 2019;95:103208.
29. Chen AC, Loiselle A, Zhou L, Baty J, Misselhorn D. Localization of peripheral pulmonary lesions using a method of computed tomography-anatomic correlation and radial probe endobronchial ultrasound confirmation. *Ann Am Thorac Soc*. 2016;13(9):1586-1592.
30. Pritchett MA, Schampaert S, de Groot JAH, Schirmer CC, van der Bom I. Cone-beam CT with augmented fluoroscopy combined with electromagnetic navigation bronchoscopy for biopsy of pulmonary nodules. *J Bronchology Interv Pulmonol*. 2018;25(4):274-282.
31. Casal RF, Sepesi B, Sagar AS, et al. Centrally located lung cancer and risk of occult nodal disease: an objective evaluation of multiple definitions of tumour centrality with dedicated imaging software. *Eur Respir J*. 2019;53(5):1802220.

32. Chang JY, Bezjak A, Mornex F. Stereotactic ablative radiotherapy for centrally located early stage non-small-cell lung cancer: what we have learned. *J Thorac Oncol*. 2015;10(4):577-585.

33. Seijo LM, de Torres JP, Lozano MD, et al. Diagnostic yield of electromagnetic navigation bronchoscopy is highly dependent on the presence of a Bronchus sign on CT imaging: results from a prospective study. *Chest*. 2010;138(6):1316-1321.

34. Weibel ER. Principles and methods for the morphometric study of the lung and other organs. *Lab Invest*. 1963;12:131-155.

35. Kurimoto N, Miyazawa T, Okimasa S, et al. Endobronchial ultrasonography using a guide sheath increases the ability to diagnose peripheral pulmonary lesions endoscopically. *Chest*. 2004;126(3):959-965.

36. Chen A, Chenna P, Loiselle A, Massoni J, Mayse M, Misselhorn D. Radial probe endobronchial ultrasound for peripheral pulmonary lesions. A 5-year institutional experience. *Ann Am Thorac Soc*. 2014;11(4):578-582.

37. Bertoletti L, Robert A, Cottier M, Chambonniere ML, Vergnon JM. Accuracy and feasibility of electromagnetic navigated bronchoscopy under nitrous oxide sedation for pulmonary peripheral opacities: an outpatient study. *Respiration*. 2009;78(3):293-300.

38. National Institutes of Health Clinical Center. PRECIsE: a prospective evaluation of the clinical utility for the ion endoluminal system. NCT03893539. ClinicalTrials.gov. National Institutes of Health; 2019. Updated December 19, 2020. https://clinicaltrials.gov/ct2/show/NCT03893539.

39. Landis JR, Koch GG. The measurement of observer agreement for categorical data. *Biometrics*. 1977;33(1):159-174.

40. Wagh A, Ho E, Murgu S, Hogarth DK. Improving diagnostic yield of navigational bronchoscopy for peripheral pulmonary lesions: a review of advancing technology. *J Thorac Dis*. 2020;12(12):7683-7690.

41. Detterbeck FC, Mazzone PJ, Naidich DP, Bach PB. Screening for lung cancer: diagnosis and management of lung cancer, 3rd ed: American College of Chest Physicians evidence-based clinical practice guidelines. *Chest*. 2013;143(5 suppl):e78S-e92S.

42. Gaga M, Powell CA, Schraufnagel DE, et al. An official American Thoracic Society/European Respiratory Society statement: the role of the pulmonologist in the diagnosis and management of lung cancer. *Am J Respir Crit Care Med*. 2013;188(4):503-507.

43. Gex G, Pralong JA, Combescure C, Seijo L, Rochat T, Soccal PM. Diagnostic yield and safety of electromagnetic navigation bronchoscopy for lung nodules: a systematic review and meta-analysis. *Respiration*. 2014;87(2):165-176.

44. Wang Memoli JS, Nietert PJ, Silvestri GA. Meta-analysis of guided bronchoscopy for the evaluation of the pulmonary nodule. *Chest*. 2012;142(2):385-393.

45. Folch EE, Labarca G, Ospina-Delgado D, et al. Sensitivity and safety of electromagnetic navigation bronchoscopy for lung cancer diagnosis: systematic review and meta-analysis. *Chest*. 2020;158(4):1753-1769.

46. Steinfort DP, Khor YH, Manser RL, Irving LB. Radial probe endobronchial ultrasound for the diagnosis of peripheral lung cancer: systematic review and meta-analysis. *Eur Respir J*. 2011;37(4):902-910.

47. Chen AC, Pastis NJ Jr, Mahajan AK, et al. Robotic bronchoscopy for peripheral pulmonary lesions: a multicenter pilot and feasibility study (BENEFIT). *Chest*. 2021;159(2):845-852.

48. Agrawal A, Hogarth DK, Murgu S. Robotic bronchoscopy for pulmonary lesions: a review of existing technologies and clinical data. *J Thorac Dis*. 2020;12(6):3279-3286.